

Published in final edited form as:

Nat Chem Biol. 2008 June ; 4(6): 373–378. doi:10.1038/nchembio.86.

Activation of the endocannabinoid system by organophosphorus nerve agents

Daniel K. Nomura¹, Jacqueline L. Blankman², Gabriel M. Simon², Kazutoshi Fujioka¹, Roger S. Issa¹, Anna M. Ward¹, Benjamin F. Cravatt², and John E. Casida^{1*}

¹*Environmental Chemistry and Toxicology Laboratory, Department of Environmental Science, Policy and Management, University of California, Berkeley, California 94720-3112, USA*

²*The Skaggs Institute for Chemical Biology and Department of Chemical Physiology, The Scripps Research Institute, 10550 North Torrey Pines Road, La Jolla, California 92037-1000, USA*

Abstract

Δ^9 -Tetrahydrocannabinol (THC), the psychoactive ingredient of marijuana, exhibits useful medicinal properties, but also undesirable side-effects. The brain receptor for THC, CB₁, is also activated by the endogenous cannabinoids anandamide and 2-arachidonylglycerol (2-AG). Augmentation of endocannabinoid signaling by blockade of their metabolism may offer a more selective pharmacological approach compared to CB₁ agonists. Consistent with this premise, inhibitors of the anandamide-degrading enzyme fatty acid amide hydrolase (FAAH) produce analgesic and anxiolytic effects without cognitive defects. In contrast, we show that dual blockade of the endocannabinoid-degrading enzymes monoacylglycerol lipase (MAGL) and FAAH by selected organophosphorus agents leads to greater than 10-fold elevations in brain levels of both 2-AG and anandamide and robust CB₁-dependent behavioral effects that mirror those observed with CB₁ agonists. Arachidonic acid levels are decreased by the organophosphorus agents in amounts equivalent to elevations in 2-AG, indicating that endocannabinoid and eicosanoid signaling pathways may be coordinately regulated in the brain.

Keywords

anandamide; 2-arachidonylglycerol; chlorpyrifos oxon; endocannabinoid; monoacylglycerol lipase; fatty acid amide hydrolase; organophosphorus

INTRODUCTION

The endogenous cannabinoid ('endocannabinoid') system consists of G-protein coupled cannabinoid receptors (CB₁ and CB₂) that bind two principal endogenous ligands, 2-arachidonylglycerol (2-AG, **1**)¹ and *N*-arachidonylethanolamine (anandamide, **2**)² (Scheme 1). Endocannabinoids regulate a diverse array of neurological (e.g. memory and motility) and metabolic (e.g. feeding and lipolysis) functions, and their levels are altered under pathophysiological conditions, including pain, anxiety, neurodegenerative disease, brain injury, and metabolic disorders^{3–9}. The signaling activity of endocannabinoids is terminated by enzymatic hydrolysis. Degradation of anandamide is principally mediated by fatty acid amide hydrolase (FAAH) *in vivo*¹⁰. In contrast, the enzymes that regulate 2-AG signaling *in vivo* remain largely unknown, although studies with cell and tissue extracts have identified

*Correspondence should be addressed to J.E.C. (ect1@nature.berkeley.edu).

multiple hydrolases for this lipid, the most prominent being monoacylglycerol lipase (MAGL) 11–13.

Cannabinoid receptors not only recognize endogenous lipid ligands but are also targets of exogenous agonists, the best known of which is Δ^9 -tetrahydrocannabinol (THC, **3**), the principal psychoactive constituent of marijuana¹⁴. THC and other CB₁ agonists produce an array of intense behavioral effects, some of which, such as pain relief, have possible therapeutic utility. However, the beneficial properties of CB₁ agonists are accompanied by a number of untoward side-effects, including hypomotility, hypothermia, and cognitive dysfunction¹⁴. CB₁ agonists have also shown abuse potential in rodents, leading to dependence and withdrawal.¹⁴ These findings raise legitimate concerns about the therapeutic potential of direct CB₁ agonists. Augmentation of endocannabinoid signaling by blockade of 2-AG and/or anandamide degradation has been proposed as an alternative therapeutic strategy that might produce a selective subset of the behavioral effects observed with direct CB₁ agonists¹⁵. Consistent with this premise, FAAH (-/-) mice or rodents treated with FAAH inhibitors possess elevated brain levels of anandamide (but not 2-AG) and exhibit analgesic, anxiolytic, and anti-depressant phenotypes without concomitant alterations in motility, cognition, or body temperature¹⁶. We speculate that this may be due to location-specific elevation in endogenous anandamide signaling tone contributing to selective modulation of endocannabinoid effects. First-generation MAGL inhibitors have also been shown to reduce pain behavior, but the limited potency of these agents required their local administration to specific brain regions⁴. MAGL (-/-) mice are not currently available, so the impact of pharmacological or genetic systemic blockade of 2-AG metabolism (or of both 2-AG and anandamide hydrolysis) has not yet been determined.

Organophosphorus (OP) nerve agents produce their primary neurotoxicity through inactivation of acetylcholinesterase (AChE). However, many of the pharmacological effects of OP agents cannot be explained by disruption of cholinergic transmission^{17,18}. Indeed, the behavioral effects induced by a sarin (**4**) homolog, isopropyl dodecylfluorophosphonate (IDFP, **5**) (Table 1), are generally reminiscent of CB₁ agonists, as noted in previous studies¹⁹ and confirmed in this investigation. These initial findings raise the provocative possibility that the non-cholinergic activities of some OP agents could be due in part to augmentation of endocannabinoid signaling. We hypothesized that blocking endocannabinoid metabolism *in vivo* would lead to an elevation in 2-AG and anandamide levels in the brain to cause full-blown cannabinoid effects that mirror direct CB₁ agonists (Scheme 1). Here we have tested this hypothesis and show that IDFP completely blocks the activity of both MAGL and FAAH *in vivo*, resulting in greater than 10-fold elevations in brain levels of 2-AG and anandamide. The profound changes in brain neurochemistry correlate with full-blown cannabinoid behavioral effects, including analgesia, hypomotility, hypothermia, and catalepsy, all of which are blocked by pharmacological or genetic disruption of the CB₁ receptor. Moreover, dramatic reductions in arachidonic acid (AA, **6**) were observed in brains from OP-treated animals, suggesting that endocannabinoids may serve as principal metabolic precursors for eicosanoid pathways in the nervous system.

RESULTS

CB₁-dependent cannabinoid behavioral effects

Within 5 min after treatment with IDFP (10 mg kg⁻¹, i.p.), mice adopted a flattened posture and remained motionless with their eyes open. This state of immobility was qualitatively reminiscent of behavioral responses elicited by direct CB₁ agonists, which motivated us to examine IDFP-treated animals in the tetrad tests for cannabinoid behaviors^{14,19}. IDFP was found to produce all four behavioral effects expected from stimulating CB₁-hypomotility, analgesia, catalepsy and hypothermia. These behavioral effects were blocked by pretreatment

with the CB₁ receptor antagonist AM251²⁰ (**7**) (Fig. 1a) and were absent in CB₁(^{-/-}) mice²¹ (Fig. 1b). These results suggested that blockade of endocannabinoid metabolism was responsible for the observed action of IDFP. The magnitude of effects observed with IDFP was similar to that with a direct CB₁ agonist, WIN55212-2 (**8**)¹⁴ (10 mg kg⁻¹, i.p.) (Supplemental Fig. 1). Using similar mouse brain membrane preparations, IDFP displaces CB₁ agonist binding in vitro with an IC₅₀ of 2 nM¹⁷, similar to its IC₅₀ for MAGL (0.8 nM) and FAAH (3 nM) (Table 1), whereas even at 30 nM it did not significantly (5 ± 9 %, n=6, p>0.05) stimulate guanosine triphosphate (**9**) binding. This suggests IDFP is not acting as a direct receptor agonist at relevant concentrations.

Disruption of endocannabinoid metabolism *in vivo*

Endocannabinoid-hydrolyzing activities were examined in brain extracts from IDFP- (10 mg kg⁻¹, i.p.) and vehicle-treated mice. This treatment level for IDFP was chosen from dose-response relationships for producing cannabinoid-like behavior¹⁹. Four h post-treatment, hydrolysis of 2-AG and anandamide was inhibited by 86 ± 1 % and 94 ± 1 %, respectively, in brain tissue from IDFP-treated animals. In contrast, no detectable inhibition of AChE was observed with IDFP in the same experiment, consistent with the absence of cholinergic toxicity. IDFP is a long chain analog of sarin with dodecyl replacing methyl, a change resulting in low AChE inhibitory potency (Table 1).

The reduced levels of endocannabinoid hydrolytic activity observed in brain tissue of IDFP-treated animals correlated with more than 10-fold increases in brain levels of both 2-AG and anandamide (Fig. 2; Supplemental Table 1). Several other changes in brain lipid chemistry were also observed in IDFP-treated animals, including elevations in additional *N*-acylethanolamines (NAEs) [e.g., *N*-palmitoyl- and *N*-oleoylethanolamines (**10** and **11**)] and monoacylglycerols [2- and 1-palmitoylglycerol (**12** and **13**) and 2- and 1-oleoylglycerol (**14** and **15**)] (Supplemental Table 1). Interestingly, AA levels were decreased by IDFP in amounts equivalent to the elevations detected for 2-AG (Fig. 2). These data establish that IDFP is a potent blocker of 2-AG and anandamide metabolism *in vivo*, leading to highly elevated brain levels of both endocannabinoids and a concurrent decrease in free AA levels.

Actions of additional OP nerve agents on the endocannabinoid system

We next considered whether other OP agents also act as inhibitors of endocannabinoid metabolic enzymes and assessed their selectivity relative to AChE. Several OPs were found to be potent *in vitro* inhibitors of brain 2-AG and anandamide hydrolytic activities (Table 1). IDFP and ethyl octylfluorophosphonate (EOFP, **16**) showed good selectivity for MAGL and FAAH compared with AChE. In contrast, paraoxon (**17**) was selective for AChE compared with the endocannabinoid hydrolases. EOFP (3 mg kg⁻¹) also elicited cannabinoid-mediated hypomotility and analgesia reversed by AM251 (Supplemental Fig. 2). Interestingly, chlorpyrifos oxon (CPO, **18**) inhibited MAGL and FAAH activity *in vitro* (Table 1) and selectively elevated 2-AG but not anandamide levels *in vivo* (at 4 mg kg⁻¹ i.p., the maximum sublethal dose) (Fig. 2, Supplemental Table 1) consistent with near-complete blockade of 2-AG hydrolytic activity (75 ± 3 %, n=4). Although certain NAE species were elevated by CPO, anandamide was not increased possibly due to incomplete inhibition of anandamide hydrolysis (82 ± 7 %, n=4). The major phosphorothionate insecticide chlorpyrifos (**19**) is not suitable for direct use as an *in vitro* hydrolase inhibitor because it requires bioactivation to CPO²². Analysis of cannabinoid behavioral effects in CPO- and chlorpyrifos-treated mice was limited by cholinergic toxicity (e.g. tremoring, lacrimation and seizures) due to blockade of AChE. Nonetheless, CPO and chlorpyrifos elicited cannabinoid-like behavior (Supplemental Fig. 3). As was observed for IDFP, treatments with CPO (4 mg kg⁻¹) and chlorpyrifos (100 mg kg⁻¹) also produced significant reductions in AA brain levels (Fig. 2, Supplemental Table 1).

Assessing the selectivity of OP nerve agents

Our finding that different classes of OP agents produced dramatic elevations in brain levels of 2-AG that were accompanied by corresponding decreases in free AA suggested a previously unrecognized cross-regulation between these metabolic pools of lipids. However, an alternative possibility was that the OP agents regulated endocannabinoid and AA levels by independent mechanisms involving the inhibition of distinct sets of hydrolytic enzymes. To explore these possibilities further, the *in vivo* selectivity of IDFP and CPO were compared by the functional proteomic method activity-based protein profiling (ABPP)^{23–25}. The ABPP probe fluorophosphonate-rhodamine (FP-Rh, **20**), which broadly labels enzymes from the serine hydrolase class, was added to brain proteomes from mice treated with vehicle, IDFP, or CPO and the enzyme activity profiles analyzed by in-gel fluorescence scanning^{26,27}. Previous ABPP studies with brain membrane proteomes have resulted in assignment of many of the FP-Rh-labeled targets visible by one-dimensional-sodium dodecylsulfate-polyacrylamide gel electrophoresis (SDS-PAGE) analysis, including FAAH, MAGL, KIAA1363, and the additional 2-AG hydrolases, ABHD6 and ABHD12 (Fig. 3). We observed that both IDFP and CPO completely blocked FP-Rh labeling of FAAH and MAGL in brain membrane or cytosolic proteomes, consistent with these enzymes contributing substantially to the 2-AG and anandamide hydrolytic activities measured with substrate assays. IDFP also targeted multiple additional serine hydrolases, including KIAA1363, ABHD6, and a 150 kDa enzyme which is probably the established OP target neuropathy target esterase (NTE)^{17, 28} (Fig. 3a).

To more comprehensively inventory the targets of IDFP and CPO, brain proteomes from mice treated with these OP agents were incubated with a biotinylated fluorophosphorus probe (FP-biotin, **21**, 5 μ M, 1 h). FP-biotin-labeled proteins were then enriched by avidin chromatography, identified by multidimensional liquid-chromatography-mass spectrometry, and their relative activity signals quantified by spectral counting. This functional proteomic method, referred to as ABPP-Multidimensional Protein Identification Technology (ABPP-MudPIT)^{13,27,29}, identified 43 brain serine hydrolase activities, most of which were unaffected by treatment with IDFP or CPO (Fig. 3b). As expected, FAAH and MAGL both showed near complete inhibition in the presence of IDFP or CPO. Consistent with the gel-based ABPP results, KIAA1363, ABHD6, and NTE were all selectively inhibited by IDFP, but not CPO. Additional targets of IDFP identified by ABPP-MudPIT included ABHD3, acyl-amino acid releasing enzyme (AARE), carboxylesterase-N (CE-N), and hormone-sensitive lipase (HSL). Serine hydrolases inhibited by CPO included not only MAGL and FAAH, but also AARE, ABHD3, CE-N, HSL and the known target AChE. Thus, IDFP and CPO were found to share only 6 common serine hydrolase targets in the brain proteome—MAGL, FAAH, AARE, ABHD3, CE-N, and HSL (Fig. 4). While it is difficult to predict the global metabolic effects of inhibiting these enzymes in parallel, these data argue that OP agents can show a rather high degree of selectivity for specific subsets of the serine hydrolase superfamily *in vivo*, with endocannabinoid-metabolizing enzymes constituting a particularly sensitive branch. Considering further that the magnitude of decrease in AA levels induced by OP agents correlated inversely with the magnitude of elevation of 2-AG levels (Fig. 2), we favor a model where complete blockade of endocannabinoid metabolism depletes free AA in the brain as this lipid builds up in the form of metabolically stabilized 2-AG.

DISCUSSION

We report herein that OP nerve agents, such as IDFP and the insecticide metabolite CPO, elicit full-blown cannabinoid behavioral effects comparable to direct agonists of the CB₁ receptor. These behaviors are correlated with greater than 10-fold elevations in brain levels of the endocannabinoids 2-AG and anandamide and complete blockade of their principal hydrolytic enzymes (MAGL and FAAH, respectively). Collectively, these data strongly support a model

where some OP agents produce many of their non-cholinergic neurobehavioral effects through hyper-stimulation of the endocannabinoid system *in vivo*.

The activity of these OP agents contrasts markedly with the selective pharmacological or genetic disruption of FAAH¹⁰, which elevates anandamide (but not 2-AG) levels in brain and promotes analgesia and anxiolysis without evidence of global CB₁ activation. This finding suggests that the OP-induced cannabinoid phenotypes are attributable either to blockade of 2-AG degradation or disruption of both 2-AG and anandamide metabolism. To discriminate between these possibilities, a more complete understanding is needed of the enzymes that degrade 2-AG *in vivo*, along with selective inhibitors for these enzymes. About 85% of total brain 2-AG hydrolytic activity can be ascribed to MAGL, with the remaining 15% being mostly mediated by two uncharacterized hydrolases, ABHD6 and ABHD12¹³. Of these enzymes, only MAGL is inhibited by both IDFP and CPO *in vivo*. We therefore conclude that the elevations in brain 2-AG levels induced by OP agents are likely due to blockade of MAGL. Since the OP agents used in this study are not completely selective for MAGL or FAAH, the inactivation of additional hydrolases could have provided a potentiating background for the dramatic CB₁-dependent behavioral effects of these compounds. It is possible that partial and selective blockade of MAGL could lead to heightened endocannabinoid activity that achieves medicinal value without producing full-blown cannabinoid effects. If other 2-AG hydrolases, such as ABHD6 or ABHD12, emerge as regulators of sub-pools of 2-AG *in vivo*, these proteins might offer an alternative pharmacological strategy to control specific endocannabinoid signaling circuits without altering bulk tissue levels of 2-AG *in vivo*¹³.

This study provides new global insights into brain lipid metabolism. For example, AA has historically been considered to be under the control of cytosolic phospholipase A₂, which releases AA from the *sn*-2 position of phospholipids in a calcium-dependent manner³⁰. However, recent studies have shown that free AA levels in brain are unaltered in cPLA₂ (-/-) mice³¹. Our findings indicate that AA in the nervous system may largely originate from endocannabinoids, and 2-AG in particular, by a pathway regulated by MAGL. Since free AA exerts many cellular effects and serves as a precursor to prostaglandins³⁰, our data suggest a provocative model where the function of the endocannabinoid and eicosanoid signaling pathways could be coordinately regulated in the nervous system.

OP toxicology has historically been ascribed to AChE inhibition, which is the principal target responsible for the acute lethality caused by OP overdose. Our proteomic analysis establishes MAGL and FAAH as additional *in vivo* targets of OP agents and demonstrates that several of the non-cholinergic OP behavioral effects are mediated by the endocannabinoid system. The interactions of IDFP and CPO with MAGL and FAAH (which have binding pockets accepting long alkyl chains) are undoubtedly through phosphorylation of the active site serine (S122 for MAGL and S241 for FAAH) conserved through the serine hydrolase superfamily^{11,16,17,24}. Other IDFP and CPO targets in brain (Fig. 4) are the previously-known KIAA1363 which hydrolyzes 2-acetyl monoalkylglycerol ether lipids in cancer cells and mice³²⁻³⁴, NTE which hydrolyzes lysophosphatidylcholine³⁵ and is associated with OP-induced delayed toxicity^{28,36}, HSL which hydrolyzes diacylglycerides and cholesteryl esters, AARE which hydrolyzes N-acetyl peptides³⁷⁻⁴⁰, and a few enzymes of unknown function (NTE-R, ABHD3 and CE-N). Whether these additional hydrolases could also influence endocannabinoid metabolism is unclear, although none of them possess substantial 2-AG hydrolytic activity¹³. Some OP agents displace CB₁ agonist binding, but do not directly influence guanosine triphosphate binding or potentiate or antagonize the effects of THC^{18,41}. These earlier findings, coupled with this study, do not support a direct effect of IDFP at relevant concentrations on the CB₁ receptor. Nonetheless, we cannot exclude the possibility that an OP might produce cannabinoid effects by a combination of blockade of endocannabinoid metabolism and direct binding to CB₁ or other cannabinoid receptors *in vivo*. Considering

further that more than 98% of the anandamide-hydrolyzing activity in mouse brain can be ascribed to FAAH¹⁰, we believe that the vast majority of the effects of the OP agents studied on the endocannabinoid system are due to the dual blockade of FAAH and MAGL. The dramatic cannabinoid phenotypes induced by combined inactivation of FAAH and MAGL underscore the surprisingly high level of tonic endocannabinoid tone that can be achieved by ablation of enzymatic degradative pathways.

A critical aspect for future endocannabinoid-based therapeutic pursuits will be to attain adequate target selectivity to achieve a beneficial subset of full-blown cannabinoid pharmacology.

METHODS

Chemicals

[³H-arachidonoyl]Anandamide (**22**) was from Perkin Elmer (Boston, MA). Analytical lipid standards were from Sigma and Alexis Biochemicals (San Diego, CA). Compounds IDFP and EOFP (>98 % pure) were synthesized in the Berkeley laboratory as reported earlier^{42,43}. CPO and chlorpyrifos were from ChemService (West Chester, PA), paraoxon from Sigma and AM251 and WIN55212-2 from Tocris Cookson Inc. (Ellisville, MO) (all >99 % purity according to the vendor).

Enzymatic and receptor assays

Brain membranes (1000 g supernatant, 100,000 g pellet) were assayed for hydrolytic activities of MAGL, FAAH, and AChE. Homogenates of frozen brain were prepared in 100 mM phosphate (pH 7.4) (AChE assays) or 50 mM Tris, 1 mM EDTA, 3 mM MgCl₂ (pH 7.4) (Tris buffer) (MAGL and FAAH assays). MAGL activity in brain membranes (10 μg protein) was assayed with 100 μM 2-AG in Tris buffer incubated for 1 h at 37°C as reported¹³ except using ethyl acetate for extractions and GC-MS for analysis of AA formation. FAAH activity was determined by a similar partitioning method⁴⁴, except with 1 μM [³H]anandamide incubated for 1 h at 37°C. AChE activity was monitored colorimetrically using 1 mM acetylthiocholine (ATCh, **23**) in phosphate buffer for 5 min at 25°C⁴⁴. The method for guanosine triphosphate binding was based on a described procedure⁴¹.

ABPP analysis

ABPP was performed by incubating mouse brain membrane and cytosolic proteomes with FP-Rh (50 μM, dimethyl sulfoxide stock) at a final concentration of 1 μM in 50 μl total reaction volume^{13,27}. Reactions were quenched after 30 min with 2X SDS-PAGE loading buffer at 90 °C, subjected to SDS-PAGE and visualized in-gel using a flatbed fluorescence scanner. For ABPP-MudPIT analysis, mouse brain membranes were prepared as described above. Membrane proteomes (1 mg protein) were then labeled with 5 μM FP-biotin in 1 ml phosphate-buffered saline for 1 h at room temperature and prepared for ABPP-MudPIT analysis as described previously^{13, 27}. MudPIT analysis of eluted peptides was carried out on a coupled Agilent 1100 LC-ThermoFinnigan LTQ MS system. All data sets were searched against the mouse IPI database using the SEQUEST search algorithm, and results were filtered and grouped with DTASELECT. Only proteins for which 3 or more spectral counts were identified on average in the control samples were considered for comparative analysis. Specifically, probe-labeled proteins were further identified by their presence in FP-treated samples with a spectral number at least 5-fold greater than that observed in “no probe” control runs (experiments performed as above, but without inclusion of FP-biotin).

Endogenous lipid analysis

For glycerol esters and fatty acids, each brain was weighed and homogenized in 3 ml of ethyl acetate and 3 ml of 100 mM phosphate buffer pH 7.4 containing 10 nmol of internal standard [(1-*O*-dodecylglycerol (**24**)]. The ethyl acetate phase was recovered and after workup the trimethylsilyl derivatives were analyzed by GC-MS¹⁹. An aliquot (1 μ l) of the trimethylsilyl derivatives was injected in the splitless mode into an Agilent Technologies model 6890N GC equipped with a DB-XLB fused-silica capillary column (30 m \times 0.25 mm \times 25 μ m) using a temperature program of 100 to 280°C at 10°C/min and held for 10 min. The mass spectra were obtained by electron impact ionization at 70 eV and an ion source temperature of 250 °C. An Agilent 5973A mass selective detector was used for total scan of *m/z* 35 to 550 for metabolomic analysis and single ion monitoring for quantitation of individual lipids. Normalization was based on brain weight and internal standard. For NAEs, each brain was weighed and homogenized in 8 ml of a chloroform:methanol:50 mM Tris pH 8.0 (2:1:1) mixture containing standards for NAE measurements [0.02 and 0.2 nmol of *d4*-anandamide (**25**) and *d4*-oleylethanolamine (**26**)]. LC-electrospray MS used an Agilent 1100-MSD SL instrument as described previously¹⁰.

Animal studies

Male albino Swiss-Webster mice (25–30 g) and male and female C57BL/6 mice (15–20 g) were from Harlan Laboratories (Indianapolis, IN). CB₁ $-/-$ mice (C57BL/6 background) to establish a breeding colony were a generous contribution from Carl Lupica and Andreas Zimmer (National Institutes of Health)²¹. Test compounds were administered ip with dimethyl sulfoxide (1 μ l/g body weight) as the carrier vehicle or dimethyl sulfoxide alone was injected as a control. Brains on removal were immediately placed on powdered dry ice and held at -80° C until analyzed. OP-treated mice were examined for possible cannabinoid-type hypomotility, analgesia, catalepsy and hypothermia¹⁰ avertable by AM251. Motility was assessed by placing each mouse in a clear box [46 \times 25 \times 22 cm (l \times w \times h)] marked on the floor with 7 cm square grids. The number of grids traversed by the hind paws was counted for the period of 15–20 min following the ip treatments. Analgesia was then determined by the tail immersion assay, where each mouse was hand-held with 1 cm of the tip immersed into a water bath at 56°C for up to 20 sec and the latency period for the animal to withdraw its tail was scored. The data were expressed as the percentage MPE equal to 100 \times (postinjection latency – preinjection latency)/(20 – preinjection latency). Catalepsy was evaluated 1 h post-treatment by using the bar test, in which the front paws of each mouse were placed on a rod (0.75 cm diameter) elevated 4.5 cm above the surface. Mice that remained motionless with their paws on the bar for 20 s (with the exception of respiratory movements) were scored as cataleptic¹⁰. Hypothermia was assessed 1 h post-treatment using a rectal thermometer and expressed as difference (Δ °C) compared to the pretreatment temperature (36–37 °C) for the same mouse¹⁰. Catalepsy was statistically analyzed using the Mann-Whitney U-test and hypothermia, analgesia and hypomotility with a Student's unpaired t-test.

Supplementary Material

Refer to Web version on PubMed Central for supplementary material.

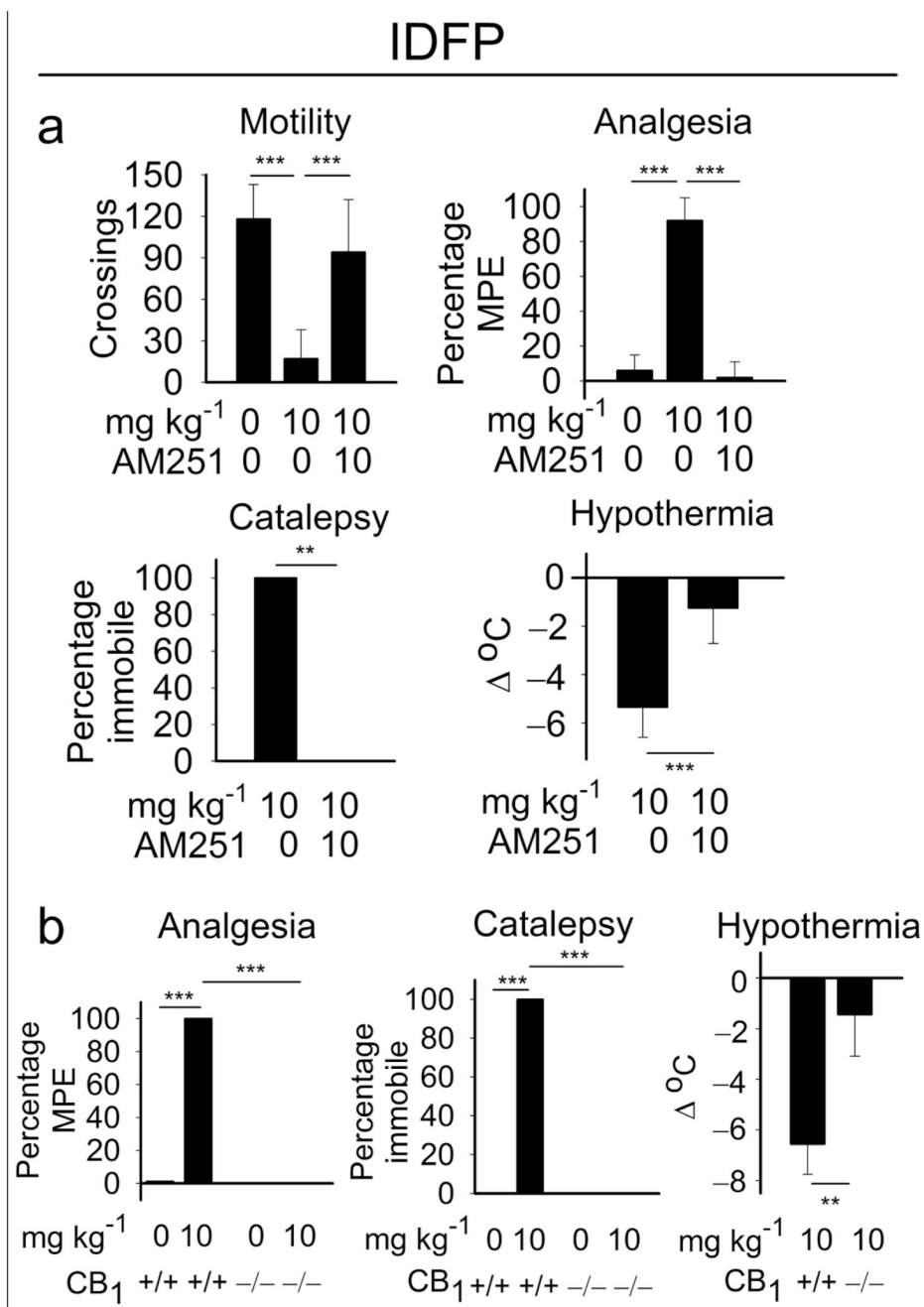
ACKNOWLEDGEMENT

This work was supported by Grants ES008762 (J.E.C.) and CA087660 (B.F.C.) from the National Institutes of Health and the University of California Toxic Substances Research and Teaching Program (D.K.N.). We thank our University of California, Berkeley colleagues Hei-Sook Sul and Maryam Ahmadian for equipment in hypothermia experiments, Rita Nichiporuk and Ulla Andersen for advice in the mass spectrometry studies and Kathleen Durkin and Tami Clark for graphical assistance. James Burston, Jenny Wiley and Aron Lichtman of Virginia Commonwealth University (Richmond, VA) provided the data on guanosine triphosphate binding.

REFERENCES

1. Sugiura T, et al. 2-Arachidonoylglycerol: a possible endogenous cannabinoid receptor ligand in brain. *Biochem. Biophys. Res. Commun* 1995;215:89–97. [PubMed: 7575630]
2. Devane WA, et al. Isolation and structure of a brain constituent that binds to the cannabinoid receptor. *Science* 1992;258:1946–1949. [PubMed: 1470919]
3. Agarwal N, et al. Cannabinoids mediate analgesia largely via peripheral type 1 cannabinoid receptors in nociceptors. *Nat. Neurosci* 2007;10:870–879. [PubMed: 17558404]
4. Hohmann, et al. An endocannabinoid mechanism for stress-induced analgesia. *Nature* 2005;435:1108–1112. [PubMed: 15973410]
5. Centonze D, Finazzi-Agrò A, Bernardi G, Maccarrone M. The endocannabinoid system in targeting inflammatory neurodegenerative diseases. *Trends Pharmacol. Sci* 2007;28:180–187. [PubMed: 17350694]
6. Monory K, et al. The endocannabinoid system controls key epileptogenic circuits in the hippocampus. *Neuron* 2006;51:455–466. [PubMed: 16908411]
7. Matias I, Bisogno T, Di Marzo V. Endogenous cannabinoid in the brain and peripheral tissues: regulation of their levels and control of food intake. *Int. J. Obes. (Lond)* 2006;30:S7–S12. [PubMed: 16570107]
8. Di Marzo V, Petrosino S. Endocannabinoid and the regulation of their levels in health and disease. *Curr. Opin. Lipid* 2007;18:129–140.
9. Di Marzo V, Disogno T, De Petrocellis L. Endocannabinoids and related compounds: walking back and forth between plant natural products and animal physiology. *Chem. Biol* 2007;14:741–756. [PubMed: 17656311]
10. Cravatt BF, et al. Supersensitivity to anandamide and enhanced endogenous cannabinoid signaling in mice lacking fatty acid amide hydrolase. *Proc. Natl. Acad. Sci., U.S.A* 2001;98:9371–9376. [PubMed: 11470906]
11. Dinh TP, et al. Brain monoglyceride lipase participating in endocannabinoid inactivation. *Proc. Natl. Acad. Sci., U.S.A* 2002;99:10819–10824. [PubMed: 12136125]
12. Dinh TP, Kathuria S, Piomelli D. RNA interference suggests a primary role for monoacylglycerol lipase in degradation of endocannabinoid 2-arachidonoylglycerol. *Mol. Pharm* 2004;66:1260–1264.
13. Blankman JL, Simon GM, Cravatt BF. A comprehensive profile of brain enzymes that hydrolyze the endocannabinoid 2-arachidonoylglycerol. *Chem. Biol* 2007;14:1347–1356. [PubMed: 18096503]
14. Pertwee R. The diverse CB₁ and CB₂ receptor pharmacology of three plant cannabinoids: Δ^9 -tetrahydrocannabinol, cannabidiol and Δ^9 -tetrahydrocannabivarin. *Brit. J. Pharmacol* 2008;153:199–215. [PubMed: 17828291]
15. Saario SM, Laitinen JT. Therapeutic potential of endocannabinoid-hydrolysing enzyme inhibitors. *Basic Clin. Pharmacol. Toxicol* 2007;101:287–293. [PubMed: 17910610]
16. McKinney MK, Cravatt BF. Structure and function of fatty acid amide hydrolase. *Annu. Rev. Biochem* 2005;74:411–432. [PubMed: 15952893]
17. Casida JE, Quistad GB. Organophosphate toxicology: safety aspects of nonacetylcholinesterase secondary targets. *Chem. Res. Tox* 2004;17:983–998.
18. Martin BR, et al. Cannabinoid properties of methylfluorophosphonate analogs. *J. Pharmacol. Exp. Therap* 2000;293:1209–1218. [PubMed: 10945879]
19. Quistad GB, Klintonberg R, Caboni P, Liang SN, Casida JE. Monoacylglycerol lipase inhibition by organophosphorus compounds leads to elevation of brain 2-arachidonoylglycerol and the associated hypomotility in mice. *Toxicol. Appl. Pharmacol* 2006;211:78–83. [PubMed: 16310817]
20. Pertwee RG. Inverse agonism and neutral antagonism at cannabinoid CB₁ receptors. *Life Sci* 2005;76:1307–1324. [PubMed: 15670612]
21. Zimmer A, Zimmer AM, Hohmann AG, Herkenham M, Bonner TI. Increased mortality, hypoactivity, and hypoalgesia in cannabinoid CB₁ receptor knockout mice. *Proc. Natl. Acad. Sci., U.S.A* 96:5780–5785. [PubMed: 10318961]
22. Gupta, RC. *Toxicology of Organophosphate & Carbamate Compounds* Ch. 9. San Diego, CA: Elsevier Academic Press; 2006.

23. Kidd D, Liu Y, Cravatt BF. Profiling serine hydrolase activities in complex proteomes. *Biochemistry* 2001;40:4005–4015. [PubMed: 11300781]
24. Evans MJ, Cravatt BF. Mechanism-based profiling of enzyme families. *Chem. Rev* 2006;106:3279–3301. [PubMed: 16895328]
25. Barglow KT, Cravatt BF. Activity-based protein profiling for the functional annotation of enzymes. *Nat. Meth* 2007;4:822–827.
26. Leung D, Hardouin C, Boger DL, Cravatt BF. Discovering potent and selective reversible inhibitors of enzymes in complex proteomes. *Nat. Biotechnol* 2003;21:687–691. [PubMed: 12740587]
27. Li W, Blankman JL, Cravatt BF. A functional proteomic strategy to discover inhibitors for uncharacterized hydrolases. *J. Am. Chem. Soc* 2007;129:9594–9595. [PubMed: 17629278]
28. Winrow CJ, et al. Loss of neuropathy target esterase in mice links organophosphate exposure to hyperactivity. *Nat. Gen* 2003;33:477–485.
29. Jessani N, et al. A streamlined platform for high-content functional proteomics of primary human specimens. *Nat. Meth* 2005;2:691–697.
30. Siegel, GJ. *Basic Neurochemistry*. 7th Ed. Burlington, MA,; Elsevier Academic Press; 2006. Ch. 33
31. Rosenberger TA, Villacreses NE, Contreras MA, Bonventre JV, Rapoport SI. Brain lipid metabolism in the cPLA₂ knockout mouse. *J. Lipid Res* 2003;44:109–117. [PubMed: 12518029]
32. Nomura DK, et al. A brain detoxifying enzyme for organophosphorus nerve poisons. *Proc. Natl. Acad. Sci., U.S.A* 2005;102:6195–6200. [PubMed: 15840715]
33. Chiang KP, Niessen S, Saghatelian A, Cravatt BF. An enzyme that regulates ether lipid signaling pathways in cancer annotated by multidimensional profiling. *Chem. Biol* 2006;13:1041–1050. [PubMed: 17052608]
34. Nomura DK, et al. Dual roles of brain serine hydrolase KIAA1363 in ether lipid metabolism and organophosphate detoxification. *Toxicol. Appl. Pharmacol* 2008;228:42–48. [PubMed: 18164358]
35. Quistad GB, Barlow C, Winrow CJ, Sparks SE, Casida JE. Evidence that mouse brain neuropathy target esterase is a lysophospholipase. *Proc. Natl. Acad. Sci., U.S.A* 2003;100:7983–7987. [PubMed: 12805562]
36. Wu S-Y, Casida JE. Subacute neurotoxicity induced in mice by potent organophosphorus neuropathy target esterase inhibitors. *Toxicol. Appl. Pharmacol* 1996;139:195–202. [PubMed: 8685903]
37. Gross NJ. Extracellular metabolism of pulmonary surfactant: the role of a new serine protease. *Annu. Rev. Physiol* 1995;57:135–150. [PubMed: 7778861]
38. Perrier J, Durand A, Giardina T, Puigserver A. Catabolism of intracellular N-terminal acetylated proteins: involvement of acylpeptide hydrolase and acylase. *Biochimie* 2005;87:673–685. [PubMed: 15927344]
39. Haemmerle G, et al. Hormone-sensitive lipase deficiency in mice causes diglyceride accumulation in adipose tissue, muscle, and testis. *J. Biol. Chem* 2002;277:4806–4815. [PubMed: 11717312]
40. Osuga J, et al. Targeted disruption of hormone-sensitive lipase results in male sterility and adipocyte hypertrophy but not in obesity. *Proc. Natl. Acad. Sci., U.S.A* 2000;97:787–792. [PubMed: 10639158]
41. Savinainen JR, Saario SM, Niemi R, Järvinen T, Laitinen JT. An optimized approach to study endocannabinoid signaling: evidence against constitutive activity of rat brain adenosine A₁ and cannabinoid CB₁ receptors. *Br. J. Pharmacol* 2003;140:1451–1459. [PubMed: 14623770]
42. Segall Y, Quistad GB, Casida JE. Cannabinoid CB₁ receptor chemical affinity probes: methods suitable for preparation of isopropyl [11,12-³H]dodecylfluorophosphonate and [11,12-³H]dodecanesulfonyl fluoride. *Syn. Commun* 2003;33:2151–2159.
43. Wu S-Y, Casida JE. Ethyl octylphosphonofluoridate and analogs: optimized inhibitors of neuropathy target esterase. *Chem. Res. Toxicol* 8:1070–1075. [PubMed: 8605290]
44. Quistad GB, Sparks SE, Casida JE. Fatty acid amide hydrolase inhibition by neurotoxic organophosphorus pesticides. *Toxicol. Appl. Pharmacol* 2001;173:48–55. [PubMed: 11350214]

**Figure 1.**

CB₁-dependent effects of IDFP in the tetrad tests for cannabinoid behavior. **(a)** Aversion with CB₁ antagonist AM251 (10 mg kg⁻¹ ip). **(b)** Absence of IDFP effects with CB₁ ^{-/-} mice. Analgesia is scored as percentage maximum possible effect (MPE). CB₁ ^{-/-} mice have decreased activity in the open field²¹ so motility was not quantitated. Data represent mean values ± S.D. for *n*=5–12 mice/group for **(a)** and *n*=4–8 mice/group for **(b)**. Asterisks indicate significance, ***p*<0.01, ****p*<0.001.

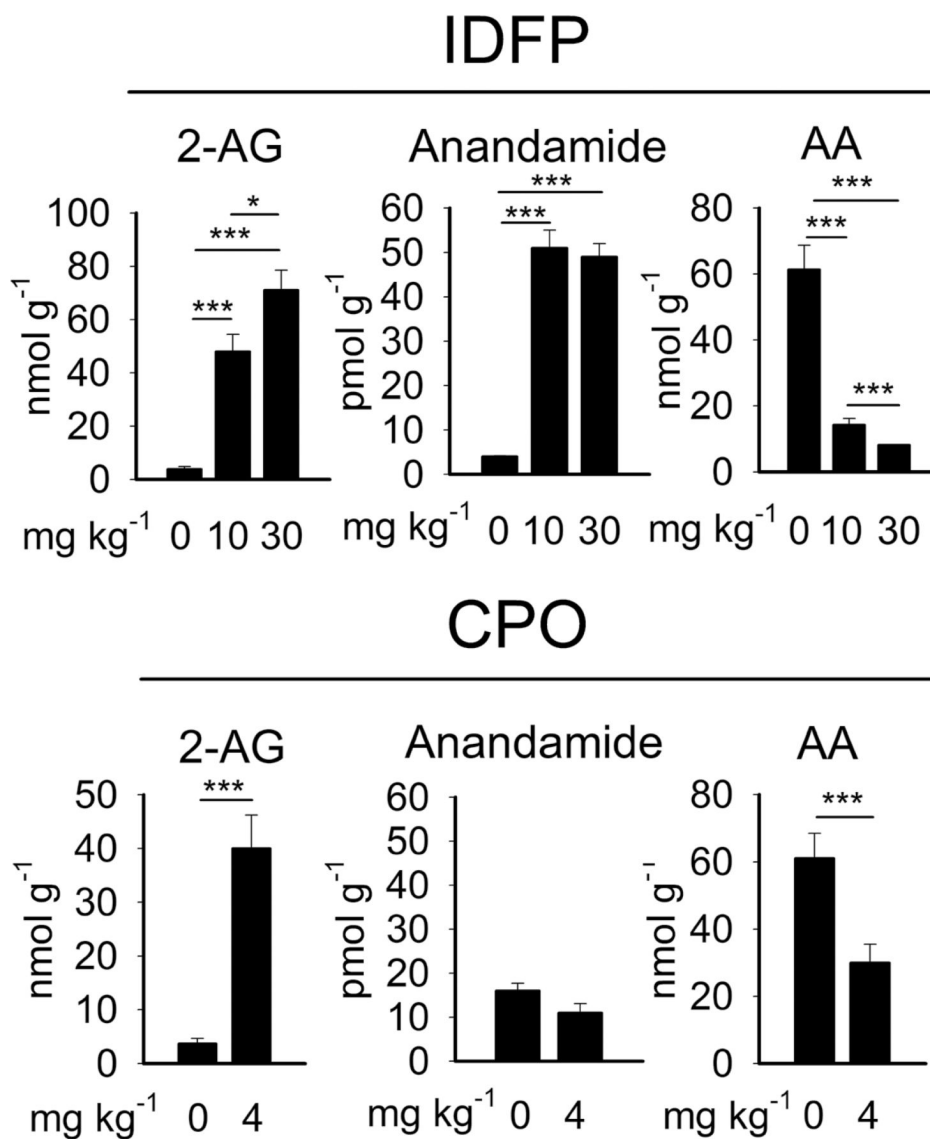
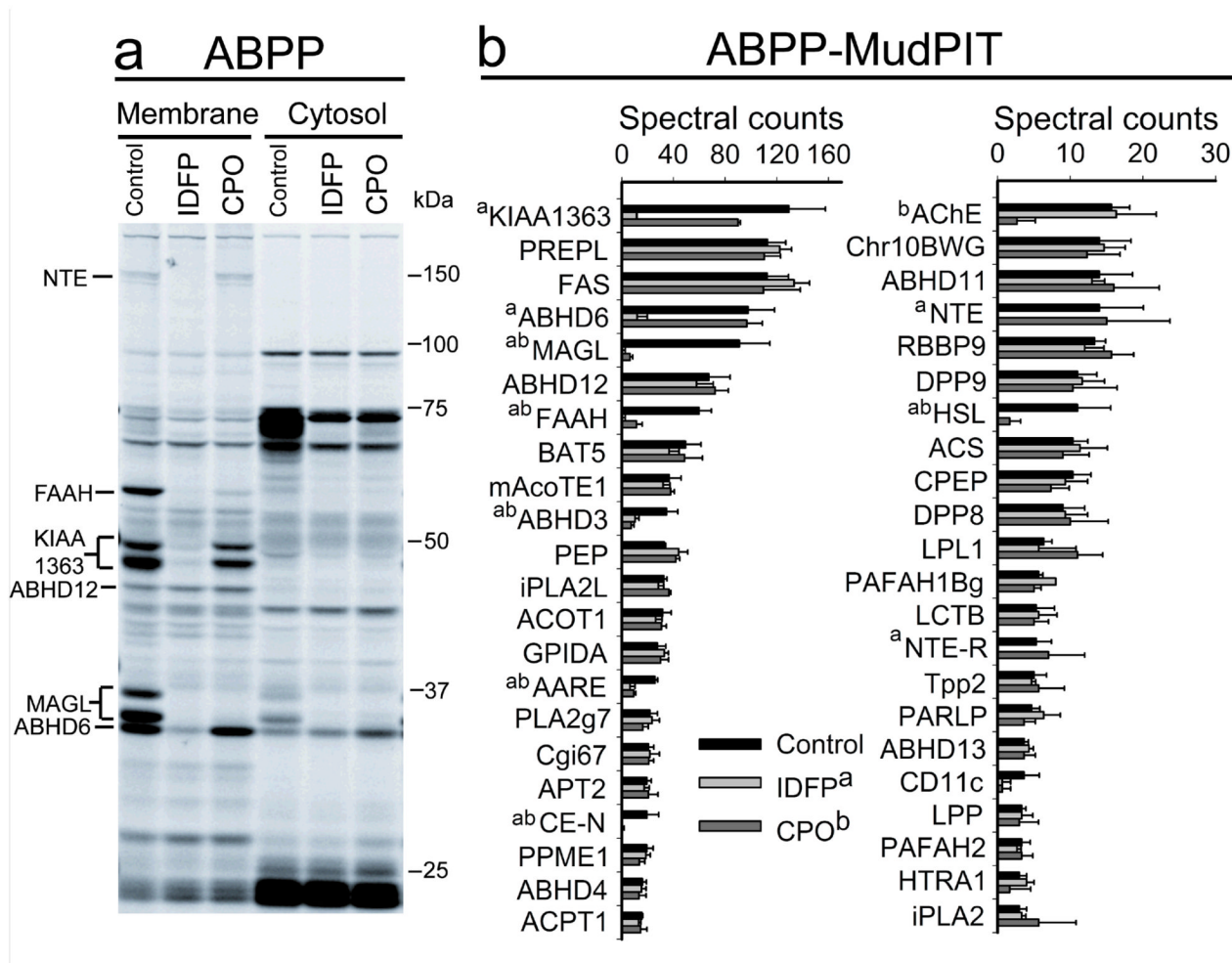


Figure 2. Effects of IDFP and CPO on endocannabinoid and AA levels in brain. The 2-AG levels are elevated by IDFP at 10 mg kg⁻¹ to the same extent at 20 min as 4 h post-treatment (data not shown). Data represent mean values \pm S.D. for $n = 8$ for control, $n = 6$ for IDFP and $n = 4$ for CPO. Asterisks indicate significance, * $p < 0.05$, *** $p < 0.001$.

**Figure 3.**

Functional proteomic analysis showing only a few brain serine hydrolases are targeted by IDFP ($10 \text{ mg kg}^{-1} \text{ ip}$) and CPO ($4 \text{ mg kg}^{-1} \text{ ip}$) at 4 h post-treatment. Assays were by gel-based ABPP and ABPP-MudPIT. Six identified OP targets are designated as to protein band(s) (left) while other OP targets (right) are either too low in abundance or not yet identified in gel-based ABPP. For ABPP-MudPIT, activities are listed in descending order of spectral counts for the controls. Abbreviations for serine hydrolase designations are listed in Supplemental Table 2. Significantly ($p < 0.05$) inhibited serine hydrolases are designated (a) for IDFP, (b) for CPO and (ab) for both. Data represent mean values \pm S.D. for $n=3$.

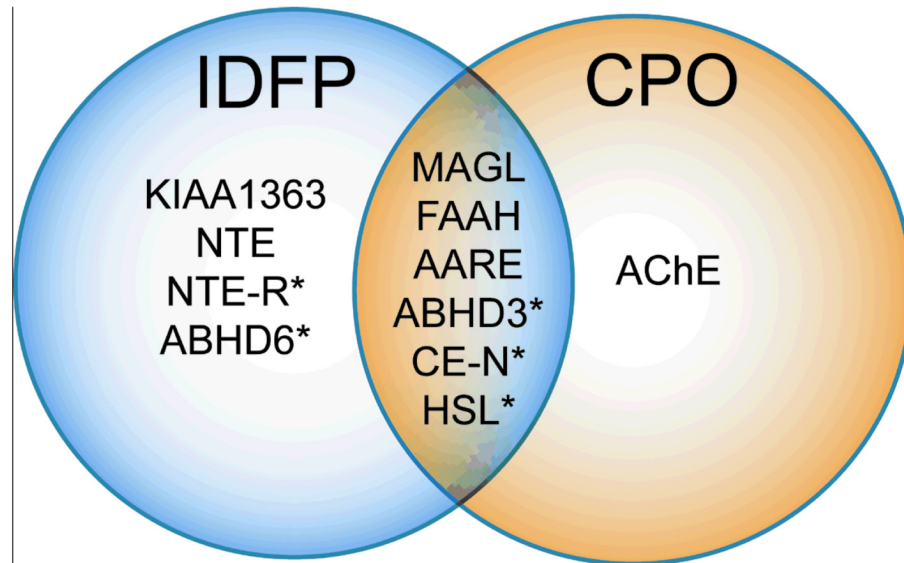
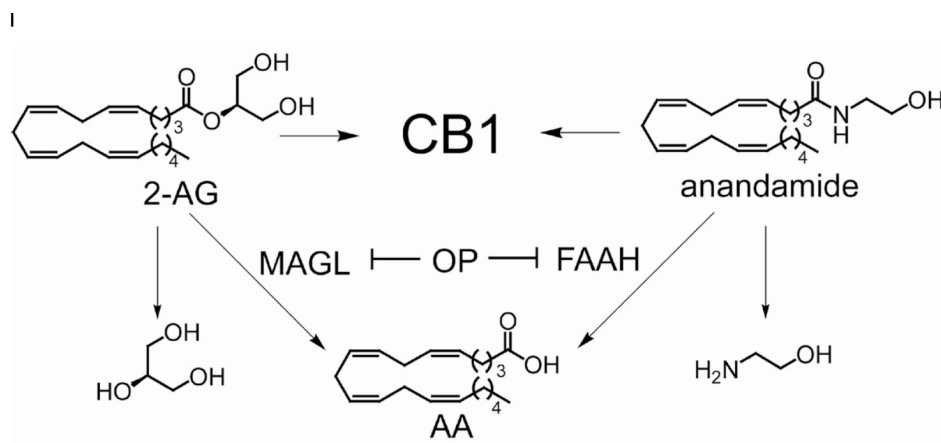
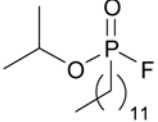
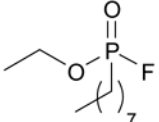
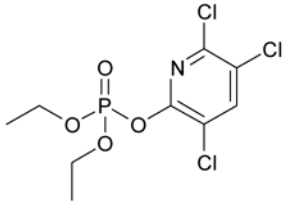
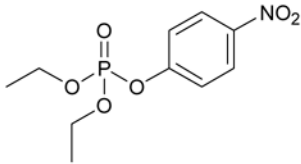


Figure 4. Proteomic targets of IDFP and CPO with significant ($p < 0.05$) *in vivo* inhibition. Asterisks indicate newly-recognized OP-sensitive targets. Data derived from Fig. 3.

**Scheme 1.**

Endocannabinoids and their primary hydrolases relative to the action of OP nerve agents. 2-AG is hydrolyzed by MAGL to glycerol (**27**) and AA. Anandamide is hydrolyzed by FAAH to ethanolamine (**28**) and AA.

Table 1
 Selective action of OP nerve agents and analogs on enzymes of the endocannabinoid versus cholinergic systems

Compound	IC ₅₀ (nM) mean ± S.D. ^a		
	Endocannabinoid		Cholinergic
	MAGL	FAAH	AChE
MAGL- and FAAH-selective versus AChE			
 11 Isopropyl dodecylfluorophosphonate (IDFP)	0.8 ± 0.2 5 ± 1 10 ± 4 1200 ± 700	3 ± 2 0.4 ± 0.2 460 ± 160 5900 ± 900	6300 ± 2300 120 ± 7 ^b 63 ± 24 13 ± 1 ^c
 Ethyl octylfluorophosphonate(EOF P)			
<u>Non-selective</u>			
 Chlorpyrifos oxon (CPO) ^b <u>AChE selective</u>			
 on Paraox			

^aMAGL, FAAH and AChE 50 % inhibitory concentrations (IC₅₀s) were determined with 2-AG, [³H]anandamide and ATCh substrates, respectively.

^bData from ref 17

^cBioactivated metabolite of the insecticide chlorpyrifos, the corresponding phosphorothionate.